

REPORT DOCUMENTATION PAGE			2	Form Approved OMB NO. 0704-0188	
<p>The public reporting burden for this collection of information is estimated to average 1 hour per response, including the time for reviewing instructions, searching existing data sources, gathering and maintaining the data needed, and completing and reviewing the collection of information. Send comments regarding this burden estimate or any other aspect of this collection of information, including suggestions for reducing this burden, to Washington Headquarters Services, Directorate for Information Operations and Reports, 1215 Jefferson Davis Highway, Suite 1204, Arlington VA, 22202-4302. Respondents should be aware that notwithstanding any other provision of law, no person shall be subject to any penalty for failing to comply with a collection of information if it does not display a currently valid OMB control number.</p> <p>PLEASE DO NOT RETURN YOUR FORM TO THE ABOVE ADDRESS.</p>					
1. REPORT DATE (DD-MM-YYYY)		2. REPORT TYPE New Reprint		3. DATES COVERED (From - To) -	
4. TITLE AND SUBTITLE Effect of amine modification on the properties of zirconium-carboxylic acid based materials and their applications as NO2 adsorbents at ambient conditions			5a. CONTRACT NUMBER W911NF-13-1-0225		
			5b. GRANT NUMBER		
			5c. PROGRAM ELEMENT NUMBER		
6. AUTHORS Amani M. Ebrahim, Teresa J. Badosz			5d. PROJECT NUMBER		
			5e. TASK NUMBER		
			5f. WORK UNIT NUMBER		
7. PERFORMING ORGANIZATION NAMES AND ADDRESSES Research Foundation CUNY - The City Col 160 Convent Avenue New York, NY 10031 -9101			8. PERFORMING ORGANIZATION REPORT NUMBER		
9. SPONSORING/MONITORING AGENCY NAME(S) AND ADDRESS (ES) U.S. Army Research Office P.O. Box 12211 Research Triangle Park, NC 27709-2211			10. SPONSOR/MONITOR'S ACRONYM(S) ARO		
			11. SPONSOR/MONITOR'S REPORT NUMBER(S) 64082-CH.7		
12. DISTRIBUTION AVAILABILITY STATEMENT Approved for public release; distribution is unlimited.					
13. SUPPLEMENTARY NOTES The views, opinions and/or findings contained in this report are those of the author(s) and should not be construed as an official Department of the Army position, policy or decision, unless so designated by other documentation.					
14. ABSTRACT Zirconium-carboxylic ligand-based porous materials modified with -NH2 groups originated either from melamine or urea were synthesized. The samples were used as adsorbents of NO2 from either dry or moist air. The surface features were analyzed using SEM, XRD, nitrogen sorption, thermal analysis and FT-IR. The incorporation of urea, which is a planar molecule, results in a highly porous crystalline materials. Melamine, a triazine compound, on the other hand obstructs the nucleation and growth of the crystals due to its interaction with metallic centers and carboxylic ligands and leads to amorphous					
15. SUBJECT TERMS UiO; Urea; Melamine; NO2 adsorption; Surface chemistry; Texture					
16. SECURITY CLASSIFICATION OF:			17. LIMITATION OF ABSTRACT UU	15. NUMBER OF PAGES	19a. NAME OF RESPONSIBLE PERSON Teresa Badosz
a. REPORT UU	b. ABSTRACT UU	c. THIS PAGE UU			19b. TELEPHONE NUMBER 212-650-6017

Report Title

Effect of amine modification on the properties of zirconium–carboxylic acid based materials and their applications as NO₂ adsorbents at ambient conditions

ABSTRACT

Zirconium–carboxylic ligand-based porous materials modified with –NH₂ groups originated either from melamine or urea were synthesized. The samples were used as adsorbents of NO₂ from either dry or moist air. The surface features were analyzed using SEM, XRD, nitrogen sorption, thermal analysis and FT-IR. The incorporation of urea, which is a planar molecule, results in a highly porous crystalline materials. Melamine, a triazine compound, on the other hand obstructs the nucleation and growth of the crystals due to its interaction with metallic centers and carboxylic ligands and leads to amorphous materials with low porosity. Water enhances the NO₂ adsorption process. Introducing Lewis basic sites by the incorporation of –NH₂ groups promotes chemical reactions on the surface. The amine (NH₂) or the carbonyl (C=O) groups in urea directly interact with NO₂ molecules in both moist and dry conditions, which leads to the formation of surface bound nitrates. In the case of melamine modified materials the hydrolysis of the terminal secondary –NH₂ creates oxygen rich functional groups that cause the formation of surface bound nitrate species.

REPORT DOCUMENTATION PAGE (SF298) (Continuation Sheet)

Continuation for Block 13

ARO Report Number 64082.7-CH

Effect of amine modification on the properties of...

Block 13: Supplementary Note

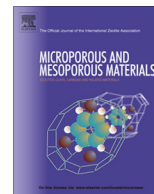
© 2014 . Published in Microporous and Mesoporous Materials, Vol. Ed. 0 188, (0) (2014), (, (0). DoD Components reserve a royalty-free, nonexclusive and irrevocable right to reproduce, publish, or otherwise use the work for Federal purposes, and to authorize others to do so (DODGARS §32.36). The views, opinions and/or findings contained in this report are those of the author(s) and should not be construed as an official Department of the Army position, policy or decision, unless so designated by other documentation.

Approved for public release; distribution is unlimited.



Contents lists available at ScienceDirect

Microporous and Mesoporous Materials

journal homepage: www.elsevier.com/locate/micromeso

Effect of amine modification on the properties of zirconium–carboxylic acid based materials and their applications as NO₂ adsorbents at ambient conditions

Amani M. Ebrahim^a, Teresa J. Bandoz^{b,*}^a Department of Chemistry, The City College of New York, 160 Convent Ave, New York, NY 10031, United States^b The Graduate School of CUNY, 160 Convent Ave, New York, NY 10031, United States

ARTICLE INFO

Article history:

Received 11 September 2013

Received in revised form 20 December 2013

Accepted 6 January 2014

Available online 13 January 2014

Keywords:

UiO

Urea

Melamine NO₂ adsorption

Surface chemistry

Texture

ABSTRACT

Zirconium–carboxylic ligand-based porous materials modified with –NH₂ groups originated either from melamine or urea were synthesized. The samples were used as adsorbents of NO₂ from either dry or moist air. The surface features were analyzed using SEM, XRD, nitrogen sorption, thermal analysis and FT-IR. The incorporation of urea, which is a planar molecule, results in a highly porous crystalline materials. Melamine, a triazine compound, on the other hand obstructs the nucleation and growth of the crystals due to its interaction with metallic centers and carboxylic ligands and leads to amorphous materials with low porosity. Water enhances the NO₂ adsorption process. Introducing Lewis basic sites by the incorporation of –NH₂ groups promotes chemical reactions on the surface. The amine (NH₂) or the carbonyl (C=O) groups in urea directly interact with NO₂ molecules in both moist and dry conditions, which leads to the formation of surface bound nitrates. In the case of melamine modified materials the hydrolysis of the terminal secondary –NH₂ creates oxygen rich functional groups that cause the formation of surface bound nitrate species.

© 2014 Elsevier Inc. All rights reserved.

1. Introduction

Metal organic frameworks have been investigated as hydrogen storage media [1–3], water oxidation catalysts [4,5], photoactive and luminescence materials [6–9] and adsorbents [10,11]. The possibility of combination of various metals and organic ligands that constitute framework of MOF units leads to microporous materials with a diversity in topology, chemistry, surface area and pore volume. Thus the ideal situation for an effective synthesis is when the “design” of MOF fits a target application. In the case of adsorption, besides textural properties, the chemical nature of metal active sites or functional groups are of paramount importance. Several efforts have been directed to introduce specific functional groups to MOF frameworks either via direct synthesis [12,13], post synthesis [14–16], grafting [17] or metal doping [18–21]. Geosten and coworkers reported a room temperature post synthetic modification of chemically and thermally stable MIL-101(Cr) and MIL-53(Al) by the incorporation of sulfoxo moieties [22]. The resulting frameworks were more acidic than the parent MOFs, and exhibited a high catalytic activity as well as high proton conductivity [22]. The removal of Hg²⁺ from water was significantly

enhanced by the post synthetic modification of MOF-199 with thiol groups using dithioglycol as a source of –SH [23].

Nitrogen dioxide (NO₂) is an acidic, corrosive, and toxic gas present in the atmosphere. The main sources of NO₂ pollution is burning of fossil fuel, emission from combustion engines and industrial wastes. Its presence in air poses a threat to the environment since it is one of the ingredients leading to a photochemical smog formation. The emission of NO₂ to the atmosphere can be eliminated either from the source or by filtration on adsorbents. MOFs, owing to their microporous nature, are considered as excellent candidates for the separation of small and toxic molecules such as NO₂ from ambient air. The most important aspect of an effective separation at ambient conditions is the ability of the material to adsorb the target molecules and eliminate the competitive effect of water when moisture is present in the system. MOFs that are widely used in the field of gas separation are HKUST-1 [24,25], MIL (Fe, Al, Cr) [26,27], MOF-5 [28–30], and UiO-66 [31–33]. The limitation in the application of HKUST-1 as an adsorbent is the complete destruction of its porosity and crystallographic structure after exposure to reactive toxic gas molecules [34]. Moreover, in humid air due to the small micropores in this system and the similarity in the size of NO₂ and water molecules [35], the competition for the adsorption sites between these two molecules can take place [36]. In addition, HKUST-1 is unstable upon a direct contact with water vapor [37,38]. In the case of MIL-100 (Fe) the addition of a foreign phase such as graphite oxide

* Corresponding author. Tel.: +1 (212) 650 6017; fax: +1 (212) 650 6107.

E-mail address: tbandosz@ccny.cuny.edu (T.J. Bandoz).

(GO) obstructed the formation of well defined crystals thus limited the ability of materials for their application as adsorbents [39].

Cavka and coworkers synthesized thermally and chemically stable UiO-66 [40]. Its stability has been linked to the highly oxophilic nature of zirconium (IV), leading to the formation of an inorganic brick $[\text{Zr}_6\text{O}_4(\text{OH})_4]$ [40]. Jasuja and co-workers synthesized a water resistant dimethyl-functionalized UiO-66. On that material, the amount of water adsorbed decreased 50%, which resulted in an increase in the uptake of CO_2 and CH_4 [41]. The incorporation of methyl groups in MOF does not introduce active sites basic enough for NO_2 adsorption and thus physical adsorption would be the predominant adsorption mechanism. Our previous study showed that UiO-type MOFs showed a promising performance as NO_2 adsorbents [42]. Nevertheless, water in the system had a negative effect on the adsorptive properties and a relatively high percentage of adsorbed NO_2 was converted to NO. It has been recently reported that UiO MOFs, especially those with BDPC as UiO-67 are unstable upon contact with water owing to the torsional strain/rotational effects in its crystalline structure [43].

Knowing that amines can enhance NO_2 and NO adsorption [44,45] and taking into account the relatively high thermal and chemical stability of UiO-66 and its analogue UiO-67 these MOFs appeared to us as good candidates for amine modification with the objective of the development of efficient NO_2 adsorbents for air filtration at ambient conditions. A post-synthetic modification was not adapted due to the rather limited reactivity (deactivated aromatic ring towards aromatic substitution) of the organic linker used, and the stability of the MOF herein. The effect of amine presence during the synthesis of zirconium based MOF on the texture and chemistry of the new materials is evaluated. The amine moiety originates from either urea or melamine. Those two compounds differ in their reactivity. The performance of the resulting materials as NO_2 reactive adsorbents at ambient conditions is linked to their surface properties.

2. Experimental

2.1. Materials

All chemicals (DMF (*N,N*-dimethylformamide 99%), BDC (Benzene-1,4-dicarboxylic acid, 98.9%), BDPC (4,4'-biphenyl-dicarboxylate 98.9%), acetone, and zirconium tetrachloride ZrCl_4) were supplied by either Sigma-Aldrich, VWR, BDH or Alfa Aesar and used without further purification.

2.1.1. Urea modified zirconium-carboxylic linkages based adsorbents

10 mmol of zirconium tetrachloride, ZrCl_4 and 10 mmol BDC were dissolved in 300 mL of *N,N*-dimethylformamide (DMF). Urea (10 mmol) was stirred in DMF separately. The solution was transferred into the ZrCl_4 /BDC solution and stirred for an additional 30 min. The reagents were transferred to a 500 mL round bottom flask, and 50 mL of DMF was added. The system was heated at 110 °C under shaking for 25 h. A resulting white product was filtered off, washed with DMF, to remove the excess of the unreacted organic linker and immersed in an acetone solution for a solvent exchange. The sample was again filtered and dried under vacuum. The sample is referred as U-ZrBDC. The same synthesis procedures were followed for the synthesis of but the materials with 4,4'-biphenyl-dicarboxylate (BDPC) used as an organic linker. The as synthesized samples is referred to as U-ZrBDPC.

2.1.2. Melamine modified zirconium-carboxylic acid linkages based adsorbents

10 mmol of zirconium tetrachloride, ZrCl_4 and 10 mmol BDC were dissolved in 350 mL of DMF. Melamine (10 mmol) was stirred

in 115 mL of ethanol separately and sonicated for 45 min. The melamine solution was then transferred to the Zr/linker solution and stirred for an additional 45 min. The reagents were transferred to a 500 mL round bottom flask. The system was heated at 115 °C under shaking for 25 h. A resulting white product was filtered off, washed with DMF, to remove the excess of the unreacted organic linker and immersed in an acetone solution for a solvent exchange. The sample was again filtered and dried under vacuum. The same synthesis procedures were followed for the synthesis of melamine-modified material, but BDPC was used as an organic linker. The as synthesized samples are referred to as M-ZrBDC and M-ZrBDPC.

2.2. Methods

2.2.1. NO_2 breakthrough capacity

The NO_2 breakthrough capacities were measured in a laboratory-scale, fixed-bed system, at room temperature, in dynamic conditions. In a typical test, 1000 ppm NO_2 in nitrogen diluted with air went through a fixed bed of an adsorbent with a total inlet flow rate of 225 mL/min. The adsorbent was well mixed with 2 mL of nonreactive glass beads (diameter 0.5–1 μm ; the beads were used to avoid pressure drop in the column) and packed into a glass column (internal diameter 9 mm). The concentrations of NO_2 and NO in the outlet gas were measured using an electrochemical sensor (RAE Systems, MultiRAE Plus PGM-50/5P). The adsorption capacity of each adsorbent was calculated in milligram per gram of adsorbent bed mg/g by integration of the area above the breakthrough curve. The tests were conducted in both moist (air was passed through a water vessel and reached relative humidity 70%) and dry conditions. The measurements were stopped at the concentrations of NO_2 and NO of 20 and 200 ppm, respectively (the limits of the gas sensors). After the breakthrough tests, all samples were exposed to a flow of carrier air only (180 mL/min) to evaluate the strength of NO_2 adsorption. The suffix -ED is added to the name of the samples after exposure to NO_2 in dry conditions, and -EM for samples after exposure to NO_2 in moist conditions.

2.2.2. Surface pH

The samples were first dried, then a 0.2 g sample of dry adsorbent was added to 10 mL of deionized water, and the suspension was stirred overnight to reach equilibrium. Then the pH was measured using Fischer scientific, Accumet Basic pH meter. The pH of the material reflects its acid-base nature and is linked to average of the number and strength of the surface acidic groups dissociating in water. It can be compared only when the same ratio of sample/water is used.

2.2.3. Adsorption of nitrogen

Nitrogen isotherms were measured at -196 °C using an ASAP 2010 (Micromeritics). Before each analysis initial and exhausted samples were dried and degassed at 120 °C. The surface area, S_{BET} the total pore volume, V_t , the micropore volume V_{mic} , (calculated from the *t*-plot), and the mesopore volume, V_{mes} , were calculated from the isotherms.

2.2.4. SEM

Scanning electron microscopy (SEM), was performed on Zeiss Supra 55 instrument with a resolution of 5 nm at 30 kV. Analyses were performed on a sample powder previously dried. For some samples, a sputter coating of a thin layer of gold was performed to avoid specimen charging.

2.2.5. XRD

To obtain crystallographic structure of the materials XRD was employed. Using standard powder diffraction procedures, the

adsorbents (fresh, and exhausted) were inserted in a mount slide as dry powder and X-ray diffraction was measured on a Philips X'Pert X-ray diffractometer using Cu K α radiation with a routine power of 1600 W (40 kV, 40 mA).

2.2.6. Thermal analysis

Thermogravimetric (TG) curves and their derivatives (DTG) were obtained using a TA Instruments thermal analyzer, Q600. The samples (initial and exhausted moist and dry) were previously dried in oven at 100 °C to remove moisture and then heated up to 1000 °C, with a heating rate 10 °C/min under a nitrogen or air flow of 100 mL/min.

2.2.7. FTIR

Fourier transform infrared (FTIR) spectroscopy was carried out using a Nicolet Magna-IR 830 spectrometer using the attenuated total reflectance method. The spectrum was generated, collected 32 times and corrected for the background noise. The experiments were done on powdered sample.

3. Results and discussion

The measured NO₂ breakthrough curves for the urea and melamine modified materials are collected in Fig. 1. In the case

M-ZrBDC exposed to NO₂ in dry conditions the NO₂ concentration rises quickly indicating a poor adsorptive performance. For U-ZrBDC, M-ZrBDPC and especially for U-ZrBDPC, the curves flatten and the breakthrough times are considerably longer. The adsorption process in moist conditions looks complex. As in dry conditions, the performance of M-ZrBDC is rather poor. Interestingly, in the case of M-ZrBDPC after the initial breakthrough the surface of this material apparently changes and more sites for NO₂ adsorption are formed. That specific “activation” also happens for U-ZrBDPC. U-ZrBDC exhibits a typical breakthrough curve and the adsorption performance is similar in moist and dry conditions. The desorption curves are steep for all samples/runs, which indicates the strong adsorption/reaction of NO₂ on the surface.

The extent of NO₂ reduction on the surface is seen on the NO release curves collected in Fig. 2. In dry conditions BDPC ligand containing materials modified either with urea or melamine are the best performing samples from the point of view of the amount of NO released. The steps on the curve for the latter sample indicate the distinct changes in the surface chemistry/texture and thus the change in the reduction of NO₂ or NO adsorption in the pore system. These changes are also visible on the NO concentration curves in moist conditions. Here the urea modified sample shows the best performance from the point of view of the amount of NO released from the surface during the NO₂ adsorption test.

The calculated NO₂ breakthrough capacities for each sample are collected in Table 1. The performance in moist conditions is much better than that in dry ones. The best adsorbents are U-ZrBDC,

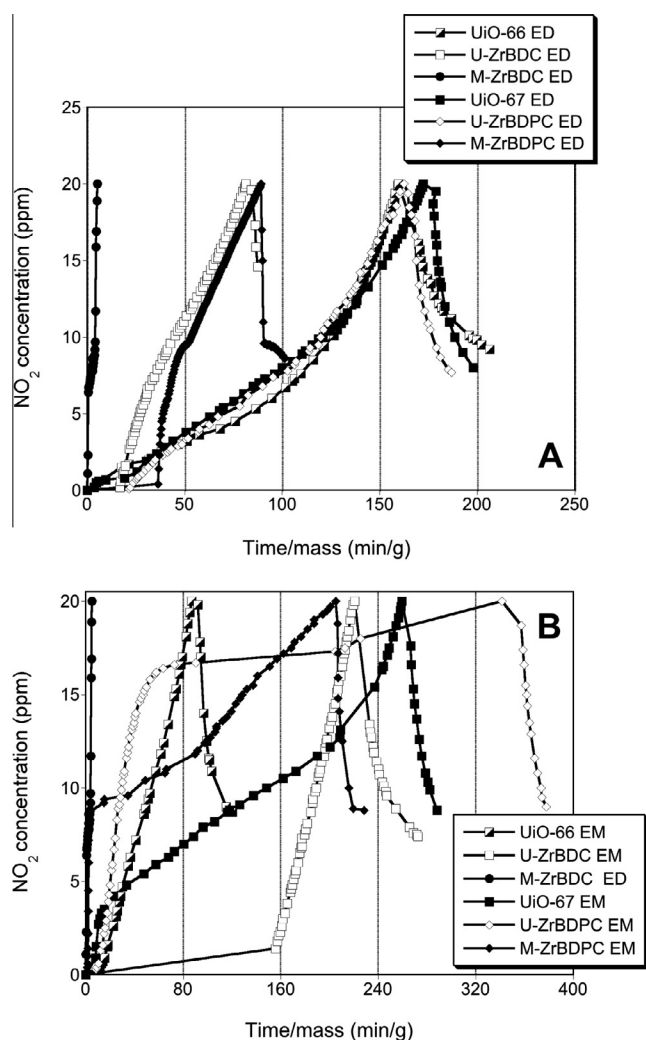


Fig. 1. NO₂ breakthrough curves for the samples studied in dry (A) and in moist (B) conditions. (Data for UiO-66 and UiO-67 is taken from Ref. [42]).

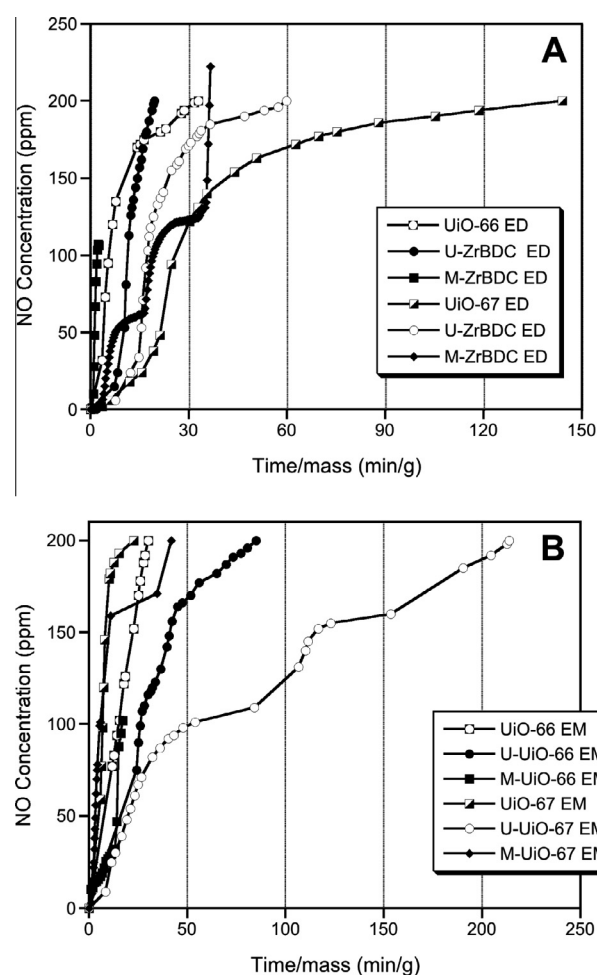


Fig. 2. NO release curves for the samples studied in dry (A) and in moist (B) conditions. (Data for UiO-66 and UiO-67 is taken from Ref. [42]).

Table 1NO₂ breakthrough capacities, percentage of NO released, water affinity and pH values before and after exposure to NO₂ in moist (EM) and dry (ED) conditions.

Samples	NO ₂ capacity (mg/g)	NO released (%)	Water adsorbed (mg _{H2O} /g _{ads})	pH	
				Initial	Exhausted
UiO-66 ED ^a	73	>30		3.00	2.90
UiO-66 EM ^a	40	~25	12	3.00	2.88
U-ZrBDC ED	37	32		2.74	2.24
U-ZrBDC EM	101	25	186	2.74	2.64
M-ZrBDC ED	3	10		2.75	2.37
M-ZrBDC EM	10	4	6	2.75	2.49
UiO-67 ED ^a	79	>30		4.78	2.90
UiO-67 EM ^a	118	<25	72	4.78	2.88
U-ZrBDPC ED	74	28		3.88	2.79
U-ZrBDPC EM	154	20	840	3.88	2.57
M-ZrBDPC ED	41	>30		3.80	3.60
M-ZrBDPC EM	93	32	70	3.80	3.54

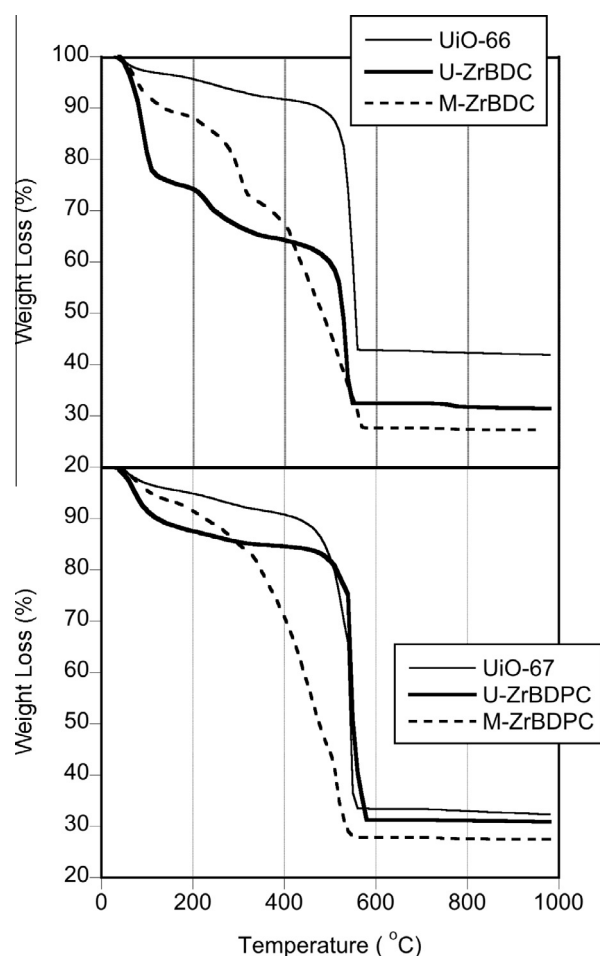
^a Data obtained from Ref. [42].

U-ZrBDPC and M-ZrBDPC exposed to NO₂ in moist conditions. There is over a 100% increase in the adsorption capacity of U-ZrBDC in moist conditions compared to for the amount adsorbed on UiO-66 (40 mg/g_{ads}) [42]. For the BDPC containing samples an increase is noticed only in moist conditions for the urea modified sample in comparison with the UiO-67 on which 118 mg NO₂/g were adsorbed [42]. In dry conditions on the unmodified sample 79 mg NO₂/g were adsorbed [34]. Therefore, in the case of BDPC containing samples the incorporation of melamine significantly worsens its performance as an NO₂ adsorbent. A similar negative effect is also found for M-ZrBDC regardless the conditions. The melamine modified BDC containing sample adsorbed 3 mg NO₂/g in dry conditions and 10 mg/g in moist conditions. On the UiO-66 73 mg NO₂/g were adsorbed in dry conditions and 40 mg/g in the moist ones [42]. The results suggest that the addition of melamine or urea significantly alters the adsorption capacity and the extent and direction of changes depend on the type of an amine modifier used. Thus the chemistry of urea seems to be more favorable for introducing beneficial surface features enhancing NO₂ adsorption. It is noteworthy that NO₂ adsorption in moist conditions is much greater than that in dry ones. This is of paramount importance in real life applications where moisture is always present in air.

Since NO formed in NO₂ surface reactions is an undesirable by-product, the percentage of NO released is summarized in Table 1. This quantity is smallest for the sample with containing BDC ligand and melamine. On this sample also the NO₂ breakthrough capacity is the lowest one. On the samples with the largest capacities the percentage of NO released is comparable to that found on the unmodified samples (~30%) [42].

The comparison of the TG curves in air for the initial samples and those modified with urea and melamine are collected in Fig. 3. As seen, the effects of modifications on the thermal stability of samples are significant. In the case of BDC containing samples a distinct weight losses between 200 and 400 °C represent the removal of modifiers in rather chemically unchanged or slightly altered forms. The rough estimation of the differences in the weight loss between the initial and modified samples suggests that about 15% or melamine and 12% of urea are present in these samples. The weight loss patterns are different for the BDPC ligand series of samples. In the case of urea modified sample high thermal stability is found and based on the shape of the curve between 500 and 550 °C it contains about 10% of urea. The chemical complexity of M-BDPC is seen in the continuous weight loss at the temperatures less than 500 °C. Then the ignition of the resulting organic phase is noticed. For all modified samples the surface hydrophilicity level increased, especially for the urea modified samples owing to the polarity of the modifier.

The incorporation of –NH₂ groups decreases the final pH of UiO (Table 1) in comparison with the unmodified samples [42].

**Fig. 3.** TG curves for the parent UiO and amine modified ZrBDC/BDPC. (Data for UiO-66 and UiO-67 is taken from Ref. [42]).

Especially that effect is seen for the BDPC containing materials where a decrease is about 1 pH unit. We link it to the protonation of the amine groups. After exposure to NO₂ a decrease in pH is dependent on the amount of NO₂ adsorbed, which suggests that acidic species are formed on the surface. Apparently presence of –NH₂ groups enhances the hydrophilicity of adsorbents. The amount of water pre-adsorbed on the urea modified samples is about 10 times greater than that on the UiO-66 and UiO-67 [42]. On the other hand, on the melamine modified samples less water is preadsorbed. An increase in hydrophilicity of the urea modified

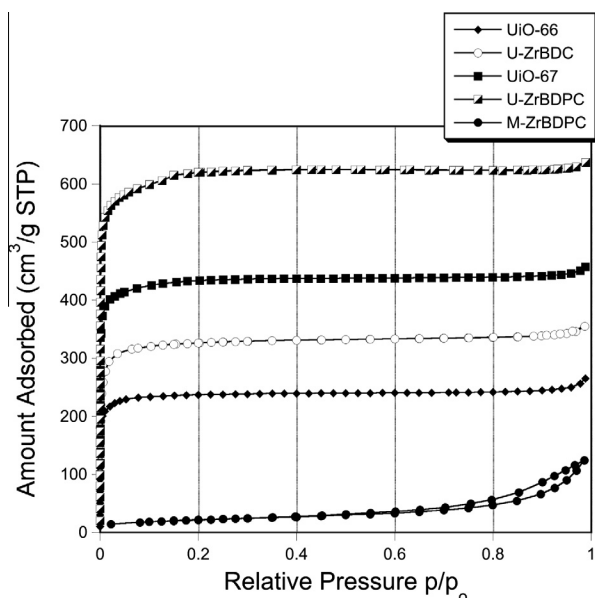


Fig. 4. Nitrogen adsorption isotherms for the initial samples and those exposed to NO₂. (Data for UiO-66 and UiO-67 is taken from Ref. [42]).

samples is owing to the nature of urea which introduces both, –NH₂ and oxygen polar groups. Melamine, on the other hand, introduces the triazine backbone, which is less polar than the carbonyl group in urea. Apparently the hydrophilicity of the surface and water in the pore system have positive effects on NO₂ adsorption on our materials.

Since UiO-66 and UiO-67 MOFs containing zirconium and carboxylic acid linkages are porous and their porosity was found crucial for NO₂ reactive adsorption [42], the porous structure of our materials was analyzed. The nitrogen adsorption isotherms and the pore size distributions for all samples before and after exposure to NO₂ are presented in Figs. 4 and 5, respectively. The parameters of the porous structure calculated from the isotherms are listed in Table 2. The positive effect of the –NH₂ modifiers on the porosity is seen for the urea modified samples and especially for U-ZrBDPC where the surface reached 2040 m²/g. This is much higher than the surface measured for UiO-67, which was 1307 m²/g [42]. For U-ZrBDC a 20% increase in the surface is found in comparison with that of UiO-66 [42]. The volume of micropores increased 48% and 17% for U-ZrBDPC and U-ZrBDC, respectively in comparison to those for UiO-67 and UiO-66. These increases in porosity must be the results of significant alterations in materials' chemistry, as discussed above based on TG curves. The higher porosity can certainly enhance the amount of NO₂ adsorbed at ambient conditions. Interestingly, the most pronounced increase in the porosity is found

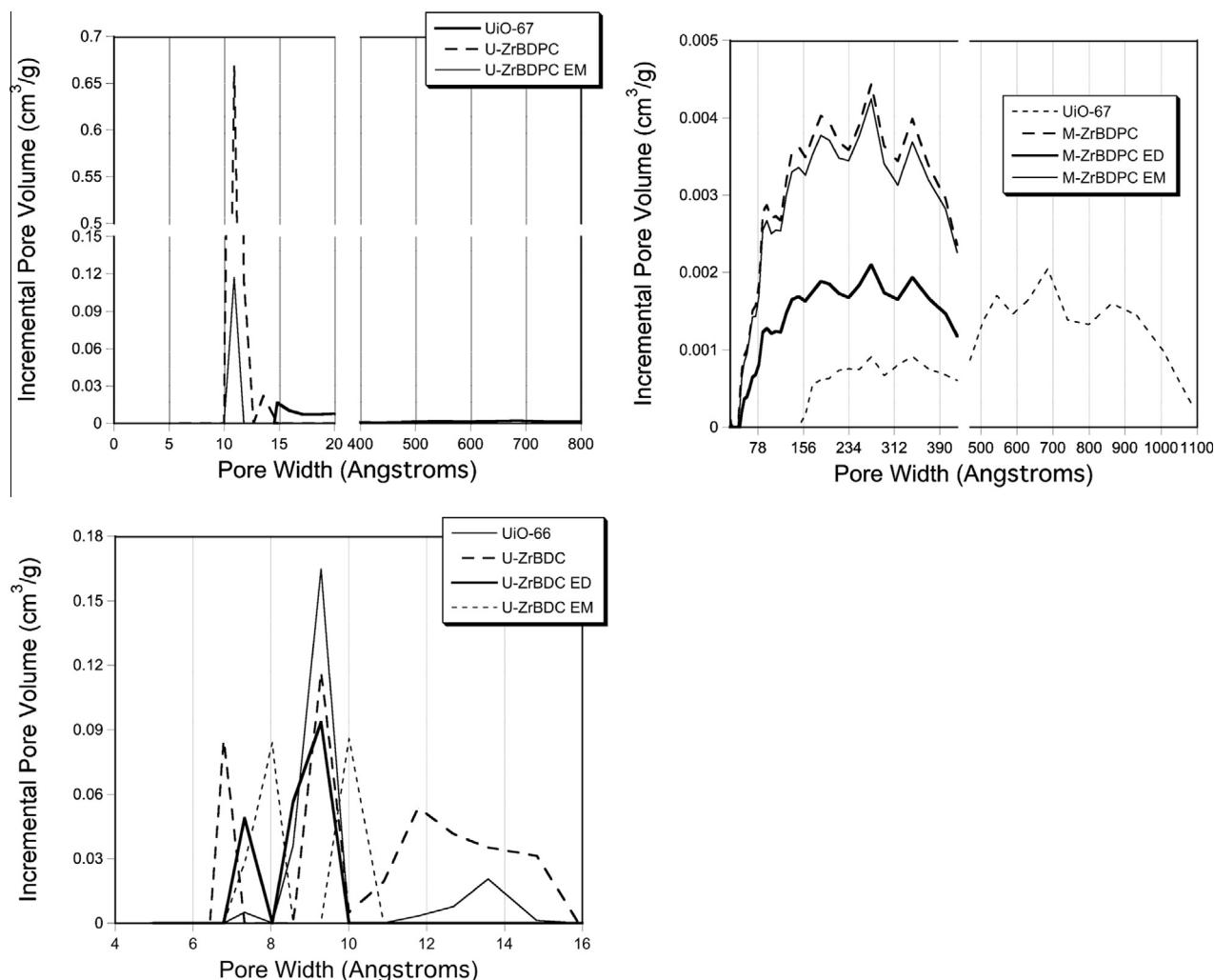


Fig. 5. Pore size distributions for the initial samples and those exposed to NO₂. U-ZrBDC is non porous after exposure to NO₂; the pores are nonexistent in the micropore range between 5 and 80 Å. (Data for UiO-66 and UiO-67 is taken from Ref. [42]).

Table 2Parameters of the porous structure derived from the nitrogen isotherms for the samples before and after exposure to NO₂.

Sample	S_{BET} [m ² /g]	V_t [cm ³ /g]	V_{mic} [cm ³ /g]	V_{meso} [cm ³ /g]	V_{mic}/V_t [%]
UiO-66 ^a	891	0.471	0.391	–	83
U-ZrBDC	1070	0.549	0.457	–	83
U-ZrBDC ED	639	0.329	0.286	0.385	87
U-ZrBDC EM	825	0.439	0.342	0.219	77
M-ZrBDC	6	0.004	0.003	0.993	80
M-ZrBDC ED	1	0.002	0.002	0.996	81
M-ZrBDC EM	3	0.006	0.0007	0.993	12
UiO-67 ^a	1372	0.707	0.608	–	86
U-ZrBDPC	2040	0.984	0.823	–	84
U-ZrBDPC ED	15	0.028	0.005	0.967	18
U-ZrBDPC EM	315	0.148	0.138	0.714	93
M-ZrBDPC	75	0.192	0.002	0.806	1.3
M-ZrBDPC ED	26	0.083	–	–	–
M-ZrBDPC EM	50	0.156	–	–	–

^a Data obtained from Ref. [42].

with an incorporation of urea. The porosity of the melamine containing samples decreased significantly compared to those for UiO-66 and UiO-67. In fact the final materials can be considered as nonporous. Apparently the presence of melamine during the synthesis prevents the formation of the UiO porous network. Interestingly, even on nonporous M-ZrBDPC the similar amount of NO₂ was adsorbed in dry conditions as that on porous U-ZrBDC, in spite of an order of magnitude higher surface area of the latter sample. This indicates that not only porosity but also surface chemistry is a very important factor affecting the adsorptive performance of this kind of materials. In the case of melamine containing samples the amount of nitrogen is the amine modifier is high and that nitrogen can be a chemically active center for reactions with NO₂/NO.

Differences in the porosity between the urea and melamine modified samples are seen not only in the volume of nitrogen adsorbed but also in the shapes of isotherms. The isotherm for M-ZrBDPC exhibits a type I hysteresis loop indicating the mesoporous nature of the sample. The shapes of the isotherms for the urea containing samples are similar to those for UiO MOFs [42]. The differences in the porosity between U-ZrBDC and U-ZrBDPC must be linked to the way the modifiers are bound to the carboxylic acid linkages. The reactions between carboxylic acids and urea should lead to the formation of imides. From both ligands, BDPC is expected to be more reactive than BDC. Owing to the larger size of those species and thus higher flexibility when present at the terminal sites of a crystalline solid, there is a high probability that those modified linkages would bind to zirconium centers either via oxygen or nitrogen groups. Thus, besides introducing a significant volume of small pores they also increase the thermal stability of the final material. The larger sizes of ligands can be responsible for some degree of porosity in amorphous M-ZrBDPC.

After NO₂ adsorption a significant decrease in the porosity is found, especially for U-ZrBDPC. That decrease is more pronounced in dry conditions than in moist ones, in spite of the much larger amount adsorbed in the latter. This trend is also true for the melamine modified samples and it suggests that water preadsorbed in the pore system preserves the adsorbents' structure from destruction via a direct attack by NO₂ molecules on the metal site [42]. Changes in the surface area and micropore volume after exposure to NO₂ are seen in PSDs (Fig. 5). Apparently, larger pores > 10 Å are the most affected ones and in fact they are the pores which can accommodate both water and NO₂ molecules.

The SEM analysis indicates that there are significant differences in the morphologies of urea and melamine containing samples (Fig. 6). While for the former samples the crystals resemble those for UiO-66 and UiO-67 [42], for the latter ones a severe alteration

in the particle geometry is observed. In fact the particles look like the agglomerates of the amorphous materials and it is consistent with the results analyzed above.

The structure of the materials and its subsequent stability after exposure to NO₂ was evaluated using X-ray diffraction (Fig. 7). As expected, the X-ray diffraction patterns for the melamine containing samples do not exhibit crystallinity similar to that of UiO-66 and UiO-67 MOFs. This is a clear indication of the amorphous nature of these materials. On the other hand, the crystallinity of the urea containing samples resembles those for the parent MOF. However, for U-ZrBDC the peak at $2\theta = 6.8^\circ$ decreases in comparison with that of the parent UiO-66. Changes are also seen on the X-ray diffraction patterns for U-ZrBDPC. The peak at $2\theta = 10^\circ$ significantly decreases in intensity and two peaks between $2\theta = 10^\circ$ and 13° change in their relative intensity. The broad peak at $2\theta = 20^\circ$ for U-ZrBDPC sharpens for the modified sample and decreases in its intensity [42]. This might be the results of the formation of new hybrid structure discussed above in which the bonds between zirconium and imides/amides are involved. Apparently the MOF units as those in UiO also exist in these materials.

Marked changes are visible on the diffraction patterns for both urea containing samples exposed to NO₂, with the exception of U-ZrBDC ED. The majority of the diffraction peaks for U-ZrBDPC ED disappears indicating the loss of crystallinity. On the other hand, the crystallinity of U-ZrBDPC EM is completely preserved. The peaks that appear on U-ZrBDPC ED between $2\theta = 42^\circ$ and 44° are also visible on the diffraction pattern for U-ZrBDPC EM, however, they are more intense for the latter sample. Additional peaks between $2\theta = 47^\circ$ and 53° are also detected for U-ZrBDPC EM. For this sample, all diffraction peaks at lower angles below $2\theta = 10^\circ$ decrease in their intensity after exposure to NO₂. The same pattern is found for U-ZrBDC after exposure to NO₂ in moist conditions. Both U-ZrBDPC EM and U-ZrBDC EM exhibit similar peaks between $2\theta = 43^\circ$ and 53° . This can be related to the interactions of the ligands/modified ligands with NO₂. Additionally, the peak at $2\theta = 26^\circ$ decreases for U-ZrBDC EM. Such changes in the intensity of all peaks indicate strong interactions of NO₂ with U-ZrBDC in the presence of moisture, which is also reflected in its high NO₂ adsorption capacity. Exposure to NO₂ does not significantly change the X-ray diffraction patterns for the melamine containing samples in either dry or moist conditions. A small peak appears around $2\theta = 22^\circ$ and can be related to the interactions of amine groups with the NO₂ molecules.

Owing to the expected chemistry involved in NO₂ removal on MOF [34,42], the formation of nitrites and nitrates is highly plausible. To investigate their formation thermal analysis was carried out. The DTG curves for the initial and exhausted samples are

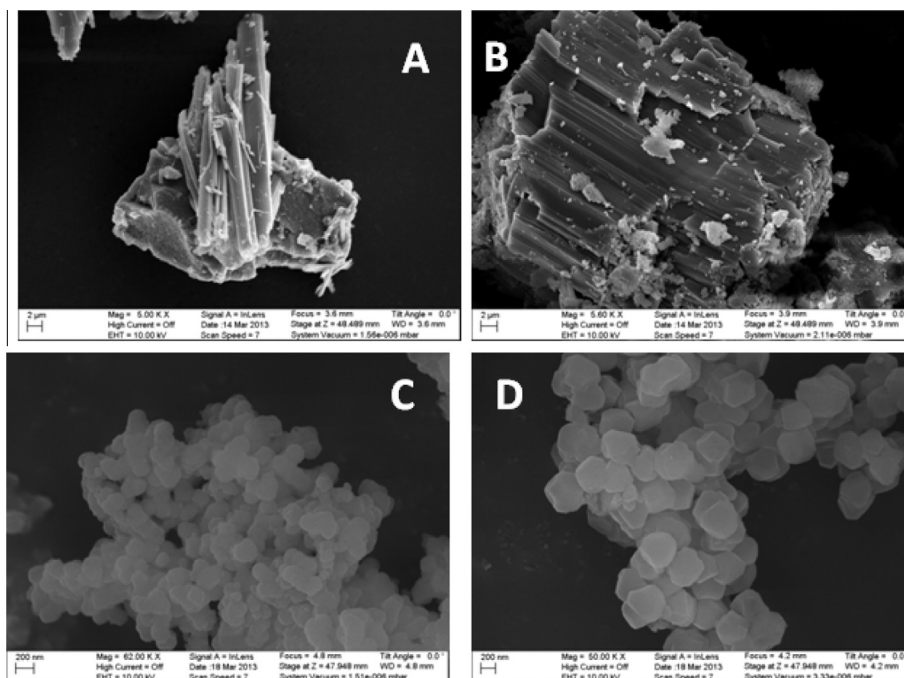


Fig. 6. SEM images for M-ZrBDC (A), M-ZrBDPC (B), U-ZrBDC (C), U-ZrBDPC (D).

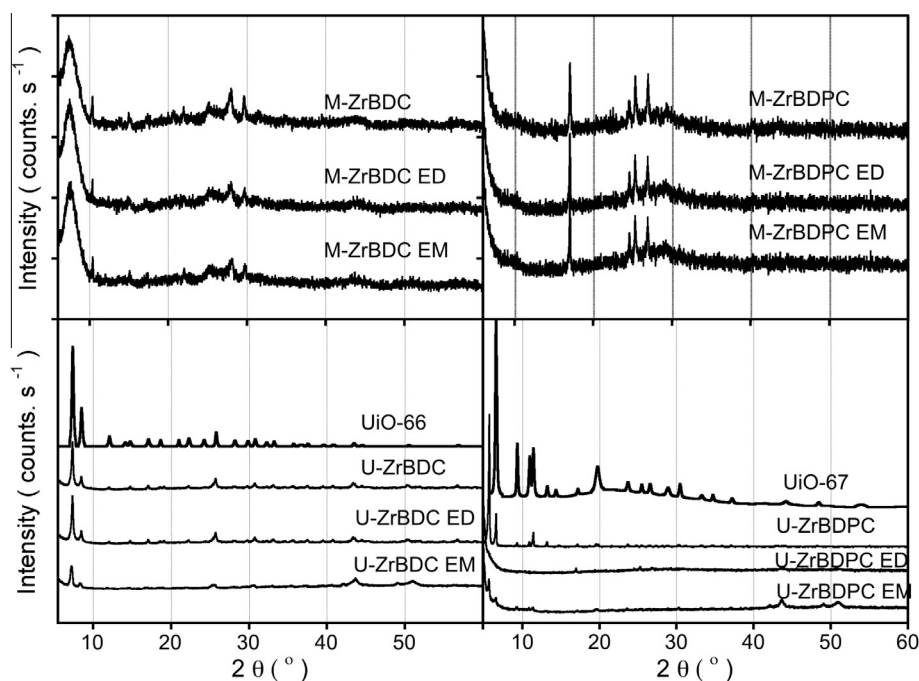


Fig. 7. XRD patterns for the initial samples and those exposed to NO₂. (Data for UiO-66 and UiO-67 is taken from Ref. [42]).

collected in Fig. 8. Typical DTG curves for Zr-based MOF are found for the urea containing samples [42]. The first peak at 100 °C represents the removal of physisorbed water. Two peaks appear between 200 and 300 °C for U-ZrBDC. The first peak is small and it is linked to the removal of residual solvent, DMF. The second peak, which is large and broad, is ascribed to the decomposition of urea and release of isocyanic acid [46–48]. The large and intense peak between 500 and 600 °C represents the decomposition/collapse of the Zr-MOF structure, by the release of ZrO₂ and the removal of the organic linker. Similar peaks are revealed for

U-ZrBDPC. A minimal difference in the derivative weight loss is found in the broad peak between 200 and 300 °C. *N,N*-dimethyl formamide (DMF), the solvent used in the synthesis decomposes in this ranges. Due to the similar chemistry of that of DMF and urea incorporated in MOF (both are carbonyl containing compounds with nitrogen groups), the two indistinctive and overlapping decomposition peaks are linked to these two compounds. More complex DTG curves are found for the M-ZrBDC/BDPC series. This complexity is related to the decomposition of the fragments that make the melamine structure. For M-ZrBDC, a rather broad peak

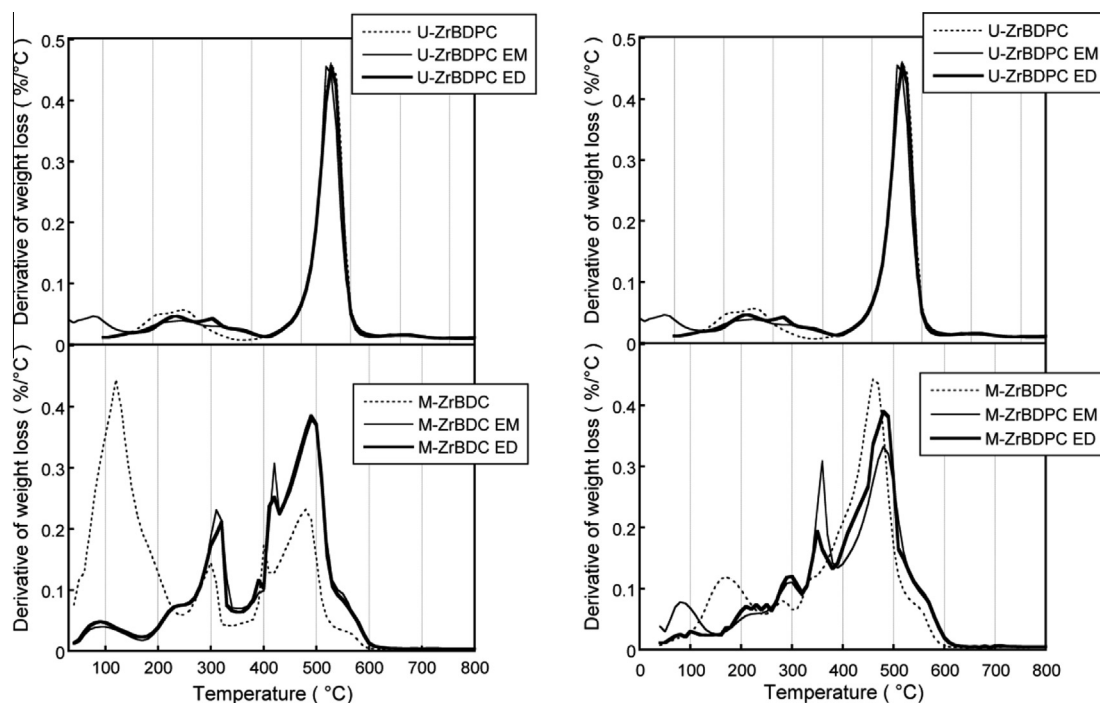


Fig. 8. DTG curves for the initial samples and those exposed to NO_2 .

between 30 and 210 °C is designated to the removal of physisorbed water and to the release of NH_3 from the $-\text{NH}_2$ fragments in melamine. The peaks between 350–400 °C and 400–450 °C are ascribed to the re-aromatization of the triazine backbone and its final degradation [49]. The peak around 470 °C represents the removal of organic linkers from their coordination with zirconium. It is interesting to note a slight overlap in the peaks corresponding to the complete degradation of the triazine backbone and in the peak corresponding to the release of organic ligands from their compounds/salts with zirconium. This suggests some degree of coordination of Zr with the triazine backbone in melamine. This process might prevent the formation of the UiO MOF network. Moreover, the decomposition temperature corresponding to the collapse and destruction of this MOF is slightly shifted to a lower temperature range. A similar trend is found in the thermal decomposition of M-ZrBDPC.

After exposure to NO_2 two small peaks, one at 200 °C and the other at 300 °C, are found on the DTG curve for U-ZrBDPC. They are linked to the decomposition of nitrates, which might be formed as a result of acid–base reaction of $-\text{NH}_2$ with NO_2 . The most significant changes in the DTG curves for the exhausted U-ZrBDC are revealed in the peak at 550 °C. The decrease in its intensity is linked to the partial destruction of the framework caused by the interactions of NO_2 with the organic linker [42]. In the case of M-ZrBDPC the broad low temperature peaks between 100 and 200 °C, which represent the removal of NH_2 from the melamine structure in the initial samples, disappear. This is associated with the consumption of the secondary $-\text{NH}_2$ in the reactions, which are responsible for the relatively high capacity of these materials in spite of its low porosity. Acid–base reactions between the amine groups and NO_2 should lead to the formation of nitrate salts. Since these species decompose between 200 and 300 °C, the weight loss associated to this process overlap with that related to the melamine degradation. The peak between 350 and 400 °C on the DTG curves for M-ZrBDPC ED and M-ZrBDPC EM is more intense in moist conditions than that in dry conditions. This peak is attributed to the decomposition of zirconium nitrates accompanied by the release of nitrogen oxide and formation of crystalline zirconia [50–53].

The FT-IR spectra for the initial and exhausted samples are collected in Fig. 9. For the urea containing samples slight changes are visible on the typical bands characteristic of UiO [42]. For U-ZrBDC (Fig. 9A) the bands in the lower region of the spectrum between 700 and 1000 cm^{-1} are more intense than those of UiO-66. These bands represent the bending vibrations of C–N, C–H and C–O. A small band at 1010 cm^{-1} is designated to the asymmetric vibration in the C–N bond and a band at approximately 1190 cm^{-1} is ascribed to the asymmetric vibration of N–H in NH_2 [54]. The band at 1350 cm^{-1} is designated to the vibration of C–N in $\text{CO}(\text{NH}_2)_2$. A strong band typical for MOF is present at 1400 cm^{-1} and represents the vibration of C–O bond in C–OH for carboxylic acids [55]. A shoulder visible at around 1430 cm^{-1} is ascribed to the ν_s of C–N bond present in urea. A weak band between 1400 and 1550 cm^{-1} represents the vibration of the C=C in the aromatic ring of the BDC linker. The band at 1600 cm^{-1} is linked to the stretching vibration of C=O in BDC linker, C–N and N–H in urea [56]. The deformation vibration band for urea carbonyl (C=O) is shown around 1700 cm^{-1} [57]. In the case of U-ZrBDPC (Fig. 9B) the main and typical bands representing this MOF remains unchanged after the urea incorporation. Briefly, the vibrations of the carboxylate group in BDPC are seen at 1290 and 1430, and 1600–1670 cm^{-1} . A weak band around 1700 cm^{-1} is related to the carbonyl group in the carbamide of urea.

The spectra for the melamine containing samples series are complex and in the case of M-ZrBDC (Fig. 9C) several bands between 3438 and 2813 cm^{-1} are due to the asymmetric stretching vibration of $-\text{NH}_2$ in melamine [58]. A strong band around 2500 cm^{-1} represents the vibrations of $-\text{C}=\text{N}$ in the triazine backbone [59]. A sharp band around 1900 cm^{-1} is attributed to the symmetric vibration of $-\text{NH}$ in secondary amine and C=C–H stretching in the ligand. Small and sharp bands between 1700 and 2500 cm^{-1} are ascribed to the hydrogen bonding between the carbonyl group in the ligand and the secondary amine in melamine. A sharp band around 1400 cm^{-1} is due to the vibration of the C=C group in the aromatic carboxylic ligand. Moreover, the small peak around 1200 cm^{-1} are related to the vibrational frequencies of $=\text{C}-\text{N}$ stemming from the aliphatic part of the triazine ring. The intense band

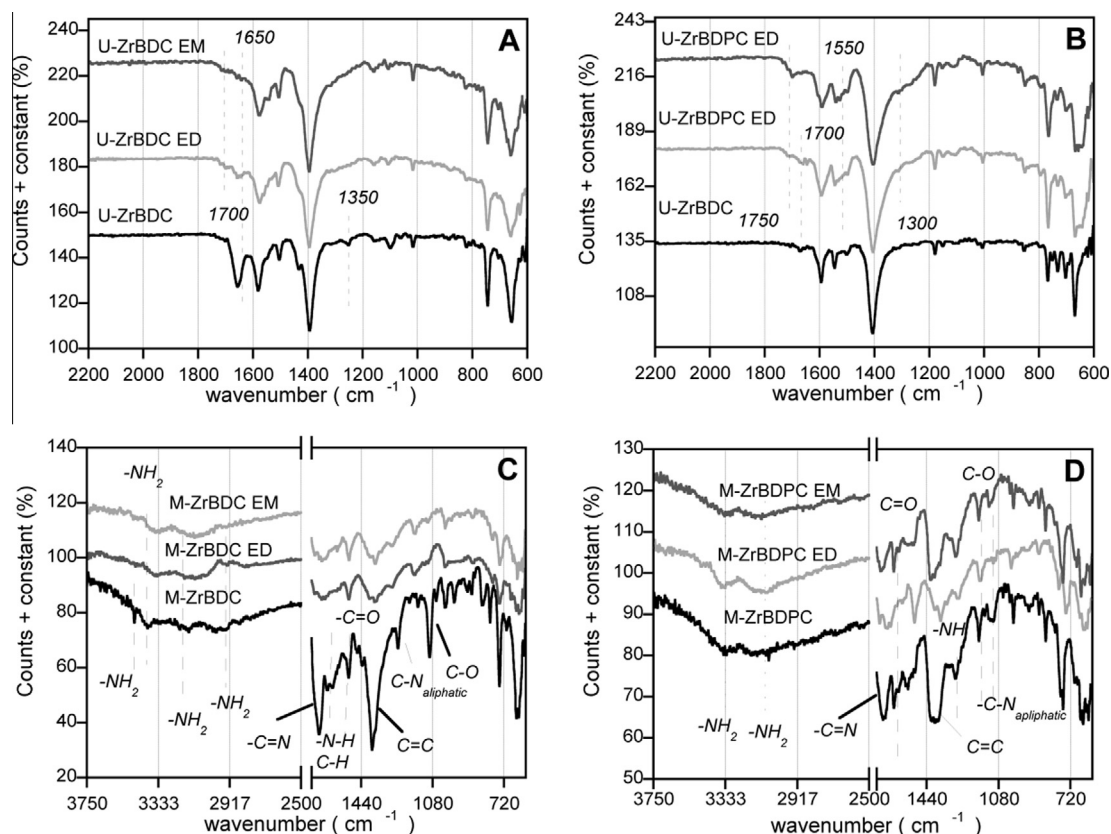


Fig. 9. FT-IR spectra for $-\text{NH}_2$ incorporated materials before (black line) and after exposure to NO_2 in dry (light grey line) and moist (dark grey line), U-ZrBDC (A), U-ZrBDPC (B), M-ZrBDC (C) and M-ZrBDPC (D).

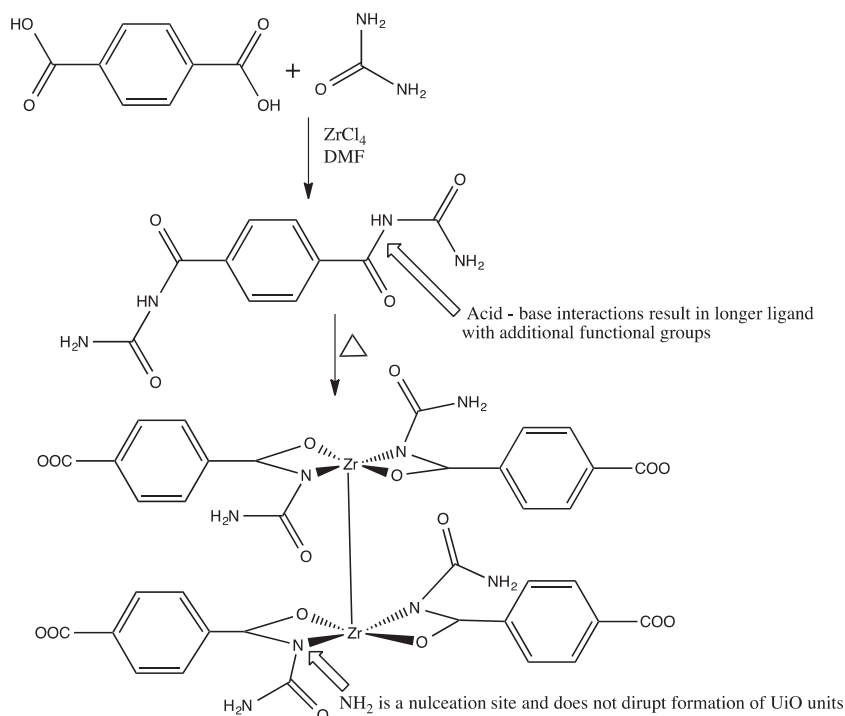


Fig. 10. Proposed schematic reaction of amine groups with carboxylic acid in the UiO unit. Formation of amide and introduction of NH-Zr metallic coordination sites in M-ZrBDC.

around 1100 cm^{-1} is ascribed to the vibration of C-N in the HN-C=N , due to the delocalization of the lone pairs on the secondary amine. Several complex bands are visible in the lower

wavelengths of the spectra. The complex bands in the region between 700 and 1090 cm^{-1} correspond to the bending and stretching vibrations of C-N , C-O and C-H in the BDC ligand and C-N as

in melamine. The band at 1090 cm^{-1} is due to the C–O stretch in the carboxylic acid. Similar bands related to the various vibrations of the functional groups and the aromatic backbone present in melamine are found on the spectra for M-ZrBDPC. Many bands between 1450 and 1750 cm^{-1} appear for this sample and they distinctly differ in their intensity from those for M-ZrBDC. In addition, the sharp band representing the vibrations of the C=O group, is less intense.

After NO_2 adsorption the FTIR spectra visibly change. A new band appears at 1700 cm^{-1} for U-ZrBDC exposed to NO_2 in dry conditions. We link it to the formation of nitrates on the surface as a result of reactive adsorption. Moreover, the band at 1650 cm^{-1} representing the deformation vibration of the urea carbonyl disappears. The importance of $-\text{NH}_2$ in urea for interactions with NO_2 is visible in the decrease in the intensity of the band at $\sim 1350\text{ cm}^{-1}$ for the exhausted samples in both moist and dry conditions. The slight shoulder located around 1450 cm^{-1} also decreases after exposure to NO_2 in either conditions. For U-ZrBDC EM a small shoulder exists on the band around 1500 cm^{-1} and can be ascribed to the interactions of the secondary amine with NO_2 molecules. The bands at 1700 and 1750 cm^{-1} are also present on the spectra for U-ZrBDPC after exposure to NO_2 , regardless the conditions. These bands represent the formation of nitrates on the MOF surface. Broadening of the band around 1550 cm^{-1} is visible and it indicates the interactions of NO_2 with the C–N and/or C–O functional groups present in either urea or the organic linker. The band at 1300 cm^{-1} also broadens after exposure to NO_2 . Drastic changes are exhibited on the spectra of the melamine containing samples after exposure to NO_2 . Majority of the peaks corresponding to the various vibrations of the functional groups and NH_2 significantly decrease in their intensity. The most pronounced decrease in the intensity of the $-\text{NH}_2$ vibrations indicate that these groups undergo chemical reactions in moist conditions. The intense band representing $-\text{C}=\text{N}$ in melamine disappears from the spectra for the exhausted samples and the band corresponding to N–H vibration decreases in its intensity. Moreover, the band of $\text{C}=\text{C}$ around 1400 cm^{-1} widens and exhibits much lower intensity. The marked changes in the spectra are also seen in the weak bands in the fingerprint region. The formation of nitrates on this sample is difficult to determine, since their bands overlap with the $-\text{NH}_2$ bands in melamine. In the case of M-ZrBDPC after exposure to NO_2 minute changes are found on the FTIR spectra owing to the relatively small amount adsorbed.

The results discussed above suggest that the planar urea molecule does not obstruct the synthesis of UiO units. In the work of Yang and coworkers, the addition of triethyl amine to Mg-based

MOF was used to increase the rate of carboxylic acid deprotonation [60]. It is well known that amines are basic enough to deprotonate acids, in this case a carboxylic acid. The ability to deprotonate a carboxylic acid with a secondary amine is dependent on the substituent group on the amine. Even though the NH_2 groups in urea are resonance stabilized with the carbonyl groups, it is expected that deprotonation of the carboxylic ligand occurs and alters the porosity of the materials, especially, in the case of materials with the BDPC linkages where more free carboxylic ligands are exposed at the terminal sites as indicated by the lower pH value of this material [42]. Moreover, these ligands are expected to react with amines forming imides. These species might increase the complexity of the linkages affecting the porosity and chemistry of the final materials. They should also increase the samples' hydrophilicity. In the case of materials with the BDC ligands modified with urea the free carboxylic ligands are not present to react with urea when the linkers are used to build the MOF network. On the other hand, during the synthesis the reactions with BDC carboxylic acid are possible and urea modified linkages are formed. By binding to ZrO_2 they introduce the heterogeneity to the pore structure and increase the porosity to a certain degree. As in the case of U-ZrBDPC, the introduction of urea and promotion of acid–base reactions certainly modify the chemistry of the final material. The structure and chemistry of the urea containing samples is visualized in Figs. 10 and 11.

The scenario must look differently in the case of melamine presence during the synthesis process. Due to its aromatic nature, and the rigid and hard to break $\text{C}=\text{N}$ bonds in the triazine, NH_2 groups apparently do not take part in the formation of MOF network. On the other hand, the results suggest that they coordinate with zirconium forming amorphous materials. Reaction of carboxylic acids with melamine also results in the precipitation of amide salts. Owing to the aromatic and basic nature of melamine the $-\text{NH}_2$ groups deprotonate the COOH moieties. Moreover it is proposed that the amine groups can be the sites of metal coordination. This observation is supported by the significant changes in the XRD patterns for the melamine modified samples. These processes prevent the formation of the UiO porous network. Additionally, the lone pairs present on the nitrogen in $\text{C}=\text{N}$ that are not conjugated with the triazine backbone are possible sites for a metallic coordination. The above scenario is summarized in Fig. 12.

Nevertheless, in spite of the lack of the developed porosity, melamine presence in the samples favors retention of NO_2 in moist conditions. Two different reactive adsorption mechanisms can take place. The hydrolysis of the secondary amines in melamine is

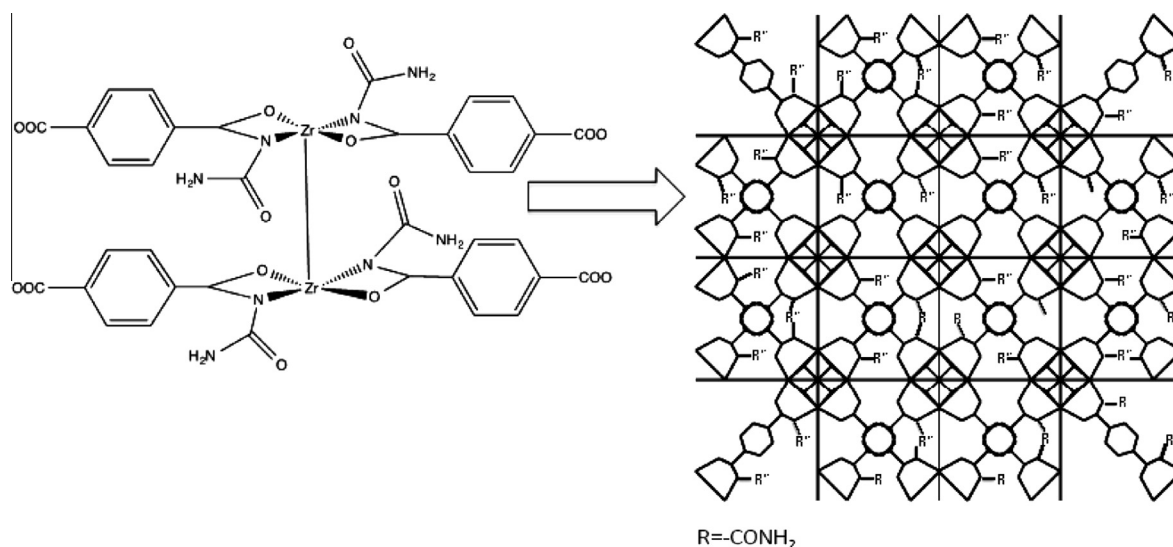
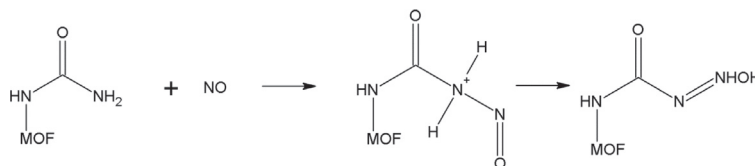


Fig. 11. Amide/imide species in U-ZrBDC.

catalyzed by the presence of water, and results in the hydroxylation of the triazine backbone by the formation of secondary –OH functional groups [61,62]. This hydrolysis reaction appears to be of paramount importance for NO₂ reactive adsorption in moist conditions, considering its high adsorption capacity measured. The interactions of NO₂ with –OH certainly leads to the formation of surface bound nitrates. The occurrence of the hydrolysis reaction is supported by a decrease in intensity of the bands for –NH₂ and the appearance of –OH vibration bands after exposure to NO₂ in moist air. The formation of hydroxyl groups is furthermore supported by the significant decrease in

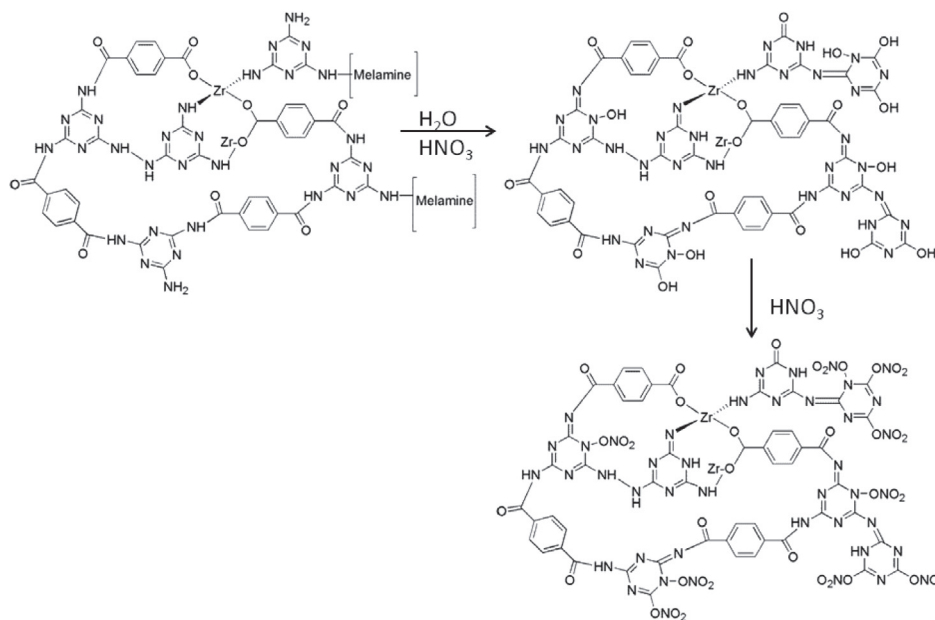
of NO during the retention process is higher in dry conditions than in moist conditions. The NH₂ groups present in these materials likely interact with NO molecules formed in surface reactions [45,64,65] and these interactions seem more favorable when moisture is present in the system. In dry conditions, further interactions/reactions of NH₂ groups with NO₂ molecules result in the release of high amounts of NO. We hypothesize that the free NH₂ groups react with NO, which leads to the formation of an intermediate protonated nitrosamine like compound. This compound then rearranges and forms of a hydrated nitramide. The reactions can be summarized below.



Schematic reaction between the urea incorporated in MOF and NO released

the intensity of the bands representing the wagging and scissoring vibration of –NH₂, especially for M-ZrBDC after exposure to NO₂ in moist conditions. Moreover, the lone pairs of electrons of the nitrogen in C=N of triazine backbone can associate with the H₂O molecules via hydrogen bonding [63]. In addition, interactions of NO₂ with the non-conjugated –NH₂ branching from the triazine backbone in melamine occurs. The reactive adsorption scenario is summarized below

In the case of urea containing samples, the hydrolysis of urea to NH₃ and CO₂ requires elevated temperatures [66] so it is not likely that the evolution of CO₂ occurs at our experimental conditions. Instead, two reactions can take place in the presence of water, which results in different products. An equilibrium acidic catalyzed hydrolysis reaction leads either to the formation of a hemiacetal by the hydrolysis of (C=O to C–(OH)₂) or the formation of ammonium carbamate [66,67]. The proposed reaction is shown below. The



Schematic diagram proposing the reaction of M-ZrBDC with HNO₃ and hydrolysis of melamine

A different mechanism in dry conditions results in a lower ability to retain NO₂ due to the delocalization of the lone pairs of electrons in –NH₂ in the aromatic ring. This delocalization decreases the strength and availability of basic active sites for NO₂ interactions. The amorphous nature of the materials, suggests that the zirconium metallic centers introduce active sites for reactive adsorption. These metallic centers interact/react with NO₂, which results in the formation of zirconium nitrates. Given that weak gas–solid interactions predominate in dry conditions, the release

hydrolysis of urea is supported by the disappearance of the carbonyl band for urea after exposure to NO₂ in moist conditions. These species decrease the ability of urea to interact with NO₂. Owing to the favorable amount of NO₂ adsorbed on the urea modified samples in moist conditions and the low content of nitrogen, the effect of urea hydrolysis, which decreases the carbonyl reactivity, does not play a major role in the NO₂ removal process. The main and most prominent reactions occurring are the Lewis acid–base reactions. These reactions are facilitated by the formation of nitric

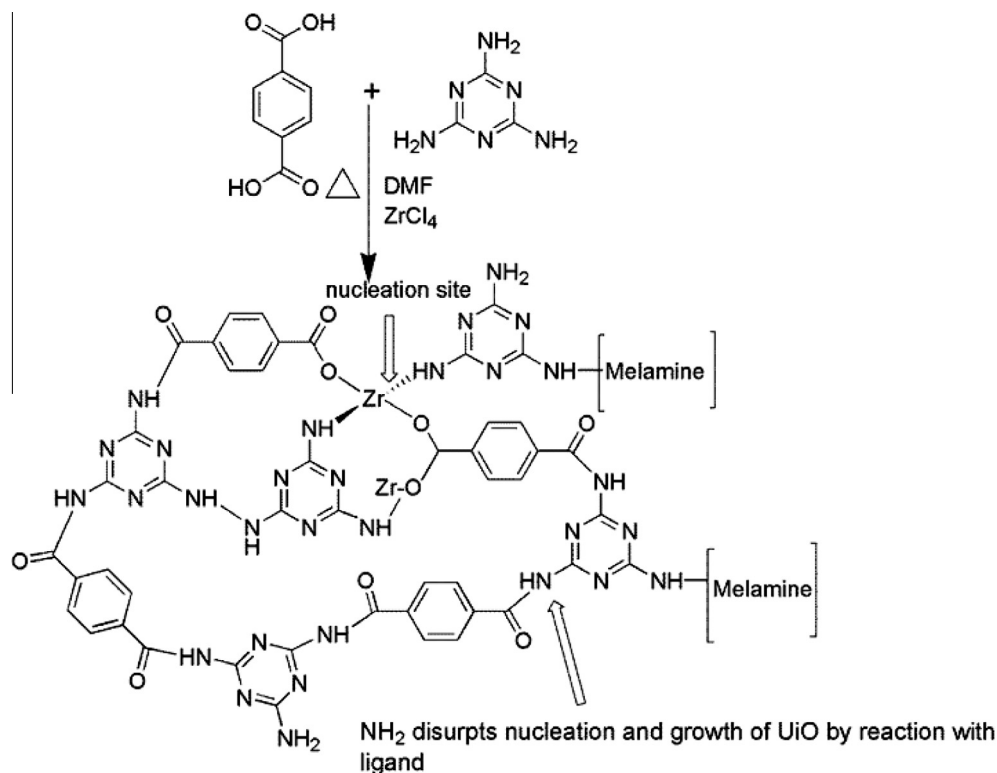
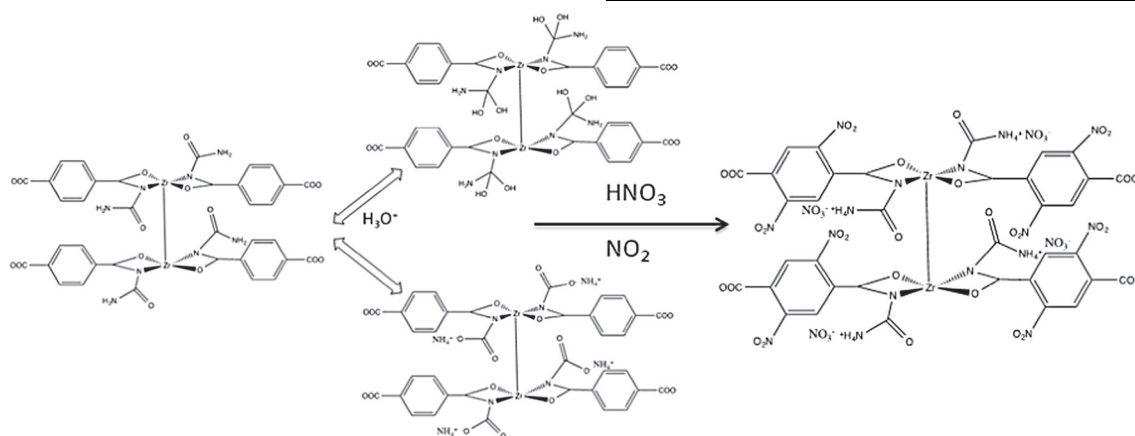


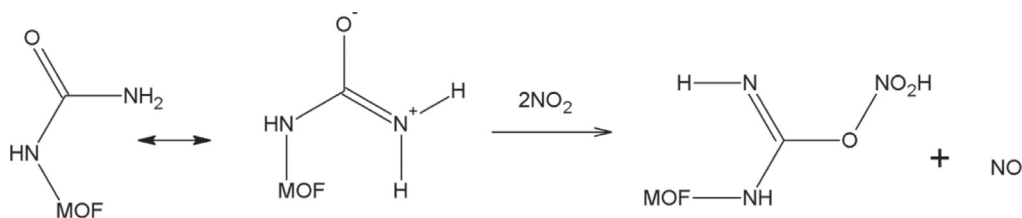
Fig. 12. Proposed schematic reaction of amine groups with carboxylic acid and introduction of $\text{NH}_2\text{-Zr}$ metallic coordination sites in M-ZrBDC.

acid via the dissolution of NO_2 in the water film. These acidic species react with -NH_2 in urea thereby forming ammonium nitrate salts. Water preferentially reacts with the amine functionalities. Apparently water has shielding effect on the UiO units, and the destruction of the framework by NO_2 molecules is less pronounced. This is an interesting observation, not in accordance with the results addressed recently for unmodified UiO-67 by Decoste and coworkers [43]. They indicated the instability of this MOF in the presence of water owing to the distortions in the framework, which weaken the Zr-O between SBU and organic linker.

In dry conditions, the -NH_2 groups either directly react via acid-base pathway with NO_2 resulting in the formation of ammonium nitrate salts or they assist the carbonyl group to react with NO_2 via resonance stabilization. Theoretical studies have shown the formation of nitrosamine by a carbonyl containing catalyzed reaction of NO_2 with amines [68–70]. We propose that the carbonyl urea can also be site for NO_2 interactions. The release of NO as a result of NO_2 complex formation with urea (C=O-NO_2), is illustrated in the following scheme:



Reaction pathway for the hydrolysis of urea in UiO and reaction of amine groups with HNO_3



Schematic diagram explaining the release of NO by the reaction between urea incorporated to the materials and NO₂

In addition to the favorable effect of the incorporation of -NH_2 to the structure of our materials whether from urea or melamine, the nitration of the benzene rings in moist conditions [42] also plays a significant role in the process of NO_2 adsorption. The nitration reactions are promoted by the sequential dissolution of NO_2 molecules in the water film, resulting in the formation of acidic species ($\text{HNO}_3/\text{HNO}_2$), which in turn causes the activation of the benzene rings for electrophilic aromatic substitution. The larger ligand (BDPC) present in both of the amine modified ZrBDPC materials (U-ZrBDPC and M-ZrBDPC) provides more “active” sites that promote these specific reactions. These additional meta positions are available for the nitration process. Additionally, the role of the larger ligand in the adsorption process via organic reactions is more pronounced in M-ZrBDPC than in M-ZrBDC, where a significantly larger amount of NO_2 is adsorbed.

4. Conclusions

Two different groups of NH_2 containing zirconium–carboxylic ligand based samples were synthesized with urea and melamine added to the components forming UiO-66 and UiO-67 MOFs. The aromatic ring in melamine leads to a mesoporous amorphous solid/salt, while planar carbamide, urea, promotes the formation of a crystalline microporous solid. The results indicate the very favorable effect of the urea incorporation to the materials on the reactive adsorption of nitrogen dioxide. Its presence increases the porosity and changes the chemistry of the final products. The surface becomes more hydrophilic and its acidity increases. The presence of -NH_2 functional groups promotes acid base reactions with NO_2 via a direct attack on -NH_2 , which result in the formation of nitrate salts. The detrimental effect of the competitive adsorption of water on UiO MOFs is eliminated, and urea significantly enhances the adsorption capacity. Water has a shielding effect on the UiO units. NO_2 dissolved in a water film forms acidic species, which interact with basic -NH_2 groups in urea. A similar effect is seen for the melamine containing samples in moist conditions. The hydrolysis of the terminal secondary -NH_2 creates oxygen rich functional groups that cause favorable interactions with NO_2 . NO released as a byproduct interacts with the amines incorporated to the material’s structure. The extent of NO adsorbed after its formation in surface reactions seems to be affected by the presence of water. In dry air a large quantity of NO is released, whereas in moist conditions the release NO is suppressed.

Acknowledgement

This study was supported by the ARO (Army Research Office) Grant W911NF-10-1-0030.

References

- [1] Q. Zhao, W. Yuan, J. Liang, J. Li, *Int. J. Hydrogen Energy* 38 (2013) 12109–13104.
- [2] D. Saha, S. Deng, *J. Phys. Chem. Lett.* 1 (2009) 73–78.
- [3] J. Purewal, D. Liu, A. Sudik, M. Veenstra, J. Yang, S. Maurer, U. Müller, D.J. Siegel, *J. Phys. Chem. C* 116 (2012) 20199–20212.
- [4] S.C. Sahoo, T. Kundu, R. Banerjee, *J. Am. Chem. Soc.* 133 (2011) 17950–17958.
- [5] C. Wang, Z. Xie, K.E. deKrafft, W. Lin, *J. Am. Chem. Soc.* 133 (2011) 13445–13454.
- [6] J.-J. Du, Y.-P. Yuan, J.-X. Sun, F.-M. Peng, X. Jiang, L.-G. Qiu, A.-J. Xie, Y.-H. Shen, J.-F. Zhu, *J. Hazard. Mater.* 190 (2011) 945–951.
- [7] S.-H. Lo, H.-K. Liu, J.-Z. Zhan, W.-C. Lin, C.C. Kao, C.-H. Lin, V. Zima, *Inorg. Chem. Commun.* 14 (2011) 1602–1605.
- [8] D. Shi, Y. Ren, H. Jiang, B. Cai, J. Lu, *Inorg. Chem. Commun.* 24 (2012) 114–117.
- [9] G.-B. Yang, Z.-H. Sun, *Inorg. Chem. Commun.* 29 (2013) 94–96.
- [10] F.A. Cabrales-Navarro, J.L. Gómez-Ballesteros, P.B. Balbuena, *J. Membr. Sci.* 428 (2013) 241–250.
- [11] K. Yang, Q. Sun, F. Xue, D. Lin, *J. Hazard. Mater.* 195 (2011) 124–131.
- [12] M. Jahan, Q. Bao, K.P. Loh, *J. Am. Chem. Soc.* 134 (2012) 6707–6713.
- [13] J.F. Eubank, H. Mouttaki, A.J. Cairns, Y. Belmabkhout, L. Wojtas, R. Luebke, M. Alkordi, M. Eddaoudi, *J. Am. Chem. Soc.* 133 (2011) 14204–14207.
- [14] S. Choi, T. Watanabe, T.-H. Bae, D.S. Sholl, C.W. Jones, *J. Phys. Chem. Lett.* 3 (2012) 1136–1141.
- [15] J. Canivet, S. Aguado, Y. Schuurman, D. Farrusseng, *J. Am. Chem. Soc.* 135 (2013) 4195–4198.
- [16] K.K. Tanabe, Z. Wang, S.M. Cohen, *J. Am. Chem. Soc.* 130 (2008) 8508–8517.
- [17] M. Jahan, Q. Bao, J.-X. Yang, K.P. Loh, *J. Am. Chem. Soc.* 132 (2010) 14487–14495.
- [18] H. Li, W. Shi, K. Zhao, H. Li, Y. Bing, P. Cheng, *Inorg. Chem.* 51 (2012) 9200–9207.
- [19] W. Dai, J. Hu, L. Zhou, S. Li, X. Hu, H. Huang, *Energy Fuels* 27 (2013) 816–821.
- [20] M. Dixit, *J. Phys. Chem. C* 116 (2012) 17336–17342.
- [21] V. Stavila, R.K. Bhakta, T.M. Alam, E.H. Majzoub, M.D. Allendorf, *ACS Nano* 6 (2012) 9807–9817.
- [22] M.G. Goesten, J. Juan-Alcañiz, E.V. Ramos-Fernandez, *J. Catal.* 281 (2011) 177–187.
- [23] F. Ke, L.-G. Qiu, Y.-P. Yuan, F.-M. Peng, X. Jiang, A.-J. Xie, Y.-H. Shen, J.-F. Zhu, *J. Hazard. Mater.* 196 (2011) 36–43.
- [24] J. Liu, Y. Wang, A.I. Benin, P. Jakubczak, R.R. Willis, M.D. LeVan, *Langmuir* 26 (2010) 14301–14307.
- [25] J. Yu, Y. Ma, P.B. Balbuena, *Langmuir* 28 (2012) 8064–8071.
- [26] T. Remy, L. Ma, M. Maes, D.E. De Vos, G.V. Baron, J.F.M. Denayer, *Ind. Eng. Chem. Res.* 51 (2012) 14824–14833.
- [27] X.Y. Chen, H. Vinh-Thang, D. Rodrigue, S. Kaliaguine, *Ind. Eng. Chem. Res.* 51 (2012) 6895–6906.
- [28] Z. Zhao, X. Ma, A. Kasik, Z. Li, Y.S. Lin, *Ind. Eng. Chem. Res.* 52 (2012) 1102–1108.
- [29] Z. Zhao, Z. Li, Y.S. Lin, *Ind. Eng. Chem. Res.* 48 (2009) 10015–10020.
- [30] J.A. Botas, G. Calleja, M. Sánchez-Sánchez, M.G. Horcajo, *Langmuir* 26 (2010) 5300–5303.
- [31] G.E. Cmarik, M. Kim, S.M. Cohen, K.S. Walton, *Langmuir* 28 (2012) 15606–15613.
- [32] Q. Yang, A.D. Wiersum, H. Jobic, V. Guillermin, C. Serre, P.L. Llewellyn, G. Maurin, *J. Phys. Chem. C* 115 (2011) 13768–13774.
- [33] H. Wu, T. Yildirim, W. Zhou, *J. Phys. Chem. Lett.* 4 (2013) 925–930.
- [34] C. Petit, B. Levasseur, B. Mendoza, T.J. Bandoz, *Microporous Mesoporous Mater.* 154 (2012) 107–112.
- [35] B. Levasseur, C. Petit, T.J. Bandoz, *ACS Appl. Mater. Interfaces* 2 (2010) 3606–3613.
- [36] A.M. Ebrahim, B. Levasseur, T.J. Bandoz, *Langmuir* 29 (2013) 6895–6902.
- [37] P. Küsgens, M. Rose, I. Senkovska, H. Fröde, A. Henschel, S. Siegle, S. Kaskel, *Microporous Mesoporous Mater.* 120 (2009) 325–330.
- [38] P.M. Schoenecker, C.G. Carson, H. Jasuja, C.J.J. Flemming, K.S. Walton, *Ind. Eng. Chem. Res.* 51 (2012) 6513–6519.
- [39] C. Petit, T.J. Bandoz, *Adv. Funct. Mater.* 21 (2011) 2108–2117.

- [40] J.H. Cavka, S. Jakobsen, U. Olsbye, N. Guillou, C. Lamberti, S. Bordiga, K.P. Lillerud, *J. Am. Chem. Soc.* 130 (2008) 13850–13851.
- [41] H. Jasuja, K.S. Walton, *J. Phys. Chem. C* 117 (2013) 7062–7068.
- [42] A.M. Ebrahim, B. Levasseur, T.J. Bandoz, *Langmuir* 29 (2012) 168–174.
- [43] J.B. DeCoste, G.W. Peterson, H. Jasuja, T.G. Glover, Y.-G. Huang, K.S. Walton, *J. Mater. Chem. A* 1 (2013) 5642–5650.
- [44] B. Levasseur, A.M. Ebrahim, T.J. Bandoz, *Langmuir* 28 (2012) 5703–5714.
- [45] E. Deliyanni, T.J. Bandoz, *Langmuir* 27 (2010) 1837–1843.
- [46] S. Désilets, P. Brousseau, D. Chamberland, S. Singh, H. Feng, R. Turcotte, K. Armstrong, J. Anderson, *Thermochim. Acta* 521 (2011) 59–65.
- [47] P.M. Schaber, J. Colson, S. Higgins, D. Thielen, B. Anspach, J. Brauer, *Thermochim. Acta* 424 (2004) 131–142.
- [48] A.M. Bernhard, D. Peitz, M. Elsener, A. Wokaun, O. Kröcher, *Appl. Catal. B* 115–116 (2012) 129–137.
- [49] G. Wang, J. Yang, *Prog. Org. Coat.* 72 (2011) 605–611.
- [50] P. Bénard, J.P. Auffrédic, D. Louër, *Powder Diffr.* 8 (1993) 39–46.
- [51] I.S. Kainarskii, L.S. Alekseenko, É.V. Degtyareva, *Refract* 8 (1967) 434–439.
- [52] B. Robertz, F. Boschini, A. Rulmont, R. Cloots, *J. Mater. Res.* 18 (2003) 1–8.
- [53] A.-M. Azad, S. Subramaniam, *Mater. Res. Bull.* 37 (2002) 85–97.
- [54] A. Ruggirello, *J. Colloid Interface Sci.* 258 (2003) 123–129.
- [55] H.R. Abid, H. Tian, H.-M. Ang, M.O. Tade, C.E. Buckley, S. Wang, *Chem. Eng. J.* 187 (2012) 415–420.
- [56] R. Qin, G. Xu, L. Guo, Y. Jiang, R. Ding, *Mater. Chem. Phys.* 136 (2012) 737–743.
- [57] L. Ning, W. De-Ning, Y. Sheng-Kang, *Polymer* 37 (1996) 3045–3047.
- [58] İ. Kaya, M. Yıldırım, *Synth. Met.* 159 (2009) 1572–1582.
- [59] M. Drozd, M.K. Marchewka, *THEOCHEM* 716 (2005) 175–192.
- [60] D.-A. Yang, H.-Y. Cho, J. Kim, S.-T. Yang, W.-S. Ahn, *Energy Environ. Sci.* 5 (2012) 6465–6473.
- [61] S. Ono, T. Funato, Y. Inoue, T. Munechika, T. Yoshimura, H. Morita, S.-I. Rengakuji, C. Shimasaki, *J. Chromatogr. A* 815 (1998) 197–204.
- [62] B. Bann, S.A. Miller, *Chem. Rev.* 58 (1958) 131–172.
- [63] A. Berge, T. Mejdell, *Polymer* 47 (2006) 3249–3256.
- [64] N. Dai, A.D. Shah, L. Hu, M.J. Plewa, B. McKague, W.A. Mitch, *Environ. Sci. Technol.* 46 (2012) 9793–9801.
- [65] M. Florent, M. Tocci, T.J. Bandoz, *Carbon* 63 (2013) 283–293.
- [66] M.M. Barmaki, M.R. Rahimpour, A. Jahanmiri, *Sep. Purif. Technol.* 66 (2009) 492–503.
- [67] J. Šubrt, E. Michalková, J. Boháček, J. Lukáč, Z. Gánovská, B. Máša, *Hydrometallurgy* 106 (2011) 12–18.
- [68] M.J. Goldman, N.A. Fine, G.T. Rochelle, *Environ. Sci. Technol.* 47 (2013) 3528–3534.
- [69] C.-L. Lv, Y.D. Liu, R.-G. Zhong, *J. Phys. Chem. A* 113 (2009) 713–718.
- [70] Z. Sun, Y.D. Liu, R.G. Zhong, *J. Phys. Chem. A* 115 (2011) 7753–7764.